Available online at www.sciencedirect.com

ScienceDirect

*Mendeleev Commun.*, 2022, **32**, 298–301

Mendeleev Communications

# A new 3D-aromatic organoboron species on the basis of $CB_6$ unit: two states of carbon hypercoordination and structural isomerism of non-classical forms

**Tatyana N. Gribanova, Ruslan M. Minyaev* and Vladimir I. Minkin**

*Institute of Physical and Organic Chemistry, Southern Federal University, 444090 Rostov-on-Don, Russian Federation. E-mail: minyaev@ipoc.sfedu.ru*

DOI: 10.1016/j.mencom.2022.05.002

**Calculations using the DFT B3LYP/6-311+G(df,2p) and wb97XD/6-311+G(df,2p) methods predict the stability of a new three-dimensional aromatic organoboron species based on the $CB_6$ unit. Derived systems containing carbon atoms in two hypercoordination states (planar hexacoordination and inverted-umbrella heptacoordination) can be used as building blocks for constructing various stable condensed systems with many hypercoordinated carbon centers.**

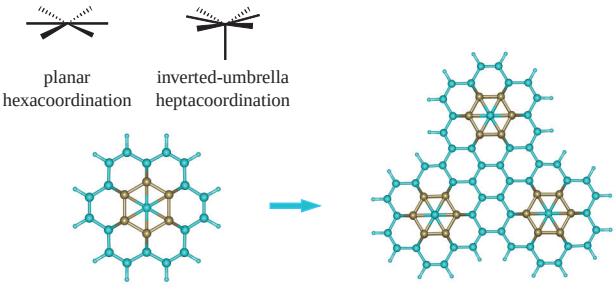


*Keywords*: organoboron compounds, quantum-chemical calculations, non-classical structures, hypercoordinated carbon, three-dimensional aromaticity.

Non-classical carbon derivatives represented by systems with nonstandard stereochemistry and hypercoordination, have attracted considerable attention not only because of their unusual structure, but also because of a wide range of potentially useful properties for applications in mechanical, optical, electronic and spintronic devices.[1–5] Theoretical and experimental studies in this area, carried out over the past few decades, have led to the discovery of many different types of non-classical forms of carbon, which have significantly transformed the concept of the valence and coordination capabilities of carbon.[1–8]

The well-studied principles of stabilization of systems with a hypercoordinated carbon can be summarized as follows: (1) binding of a hypercoordinated center to σ-donor and π-acceptor substituents, (2) its incorporation into a structurally rigid framework, (3) strong interligand bonding, (4) aromaticity of the system and (5) correspondence between the sizes of the ligand framework and the hypercoordinated atom.

The boron environment provides exceptionally suitable conditions for the stabilization of hypercoordinated forms due to the σ-donor and π-acceptor properties of boron, as well as its wide coordination capabilities, which make it possible to control the steric and electronic parameters of the framework, such as steric strain and aromaticity, in a targeted manner.[7,8]

The simplest boron-containing derivatives of hypercoordinated carbon are cyclic systems **1**,[9] **2**,[10] **3**[9,11] and **4**,[9,12] the modification of which makes it possible to design a wide range of many new non-classical carbon structures. For example, based on the actively studied cluster $CB_6^{2-}$ **2**, extended chain systems **5**,[8] sandwich derivatives of transition metals **6**[13] and multidecker metallocene complexes **7**[14] can be formed.

The next step in the study of non-classical systems is the construction of 2D and 3D crystal derivatives, which also exhibit unusual physicochemical parameters.[2] For example, 2D derivatives of planar pentacoordinated carbon are characterized by a negative Poisson's ratio,[15] and a $Be_2C$ monolayer with planar hexacoordinated carbon centers shows great potential as an anode material for high-performance lithium-ion batteries.[16]

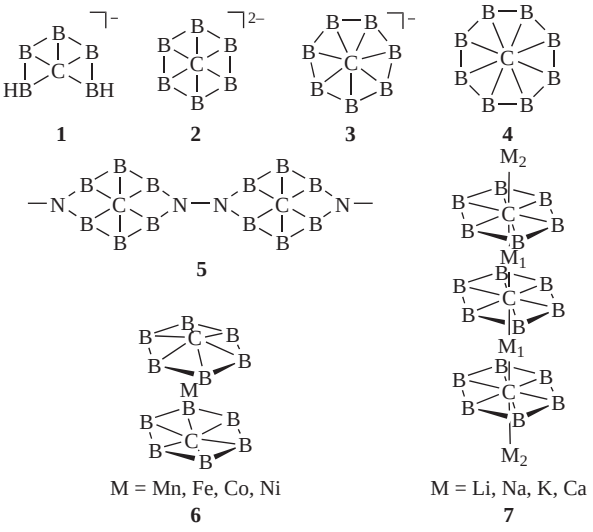


In this paper, we consider a new aspect of the chemistry of non-classical hypercoordinated carbon compounds, namely, their ability to implement several non-classical states at once in one compound. An example of a system of this type is the new organoboron system **8**, which is formed from two $CB_6$ basal cycles bonded equatorially by an annulene linker. This structure makes it possible to realize two different non-classical states of the apical carbon atoms: planar hexacoordination **8a** and inverted-umbrella heptacoordination **8b** (Figure 1).

Density functional theory (DFT) calculations were performed with the B3LYP[17] and wb97XD[18] functionals and the

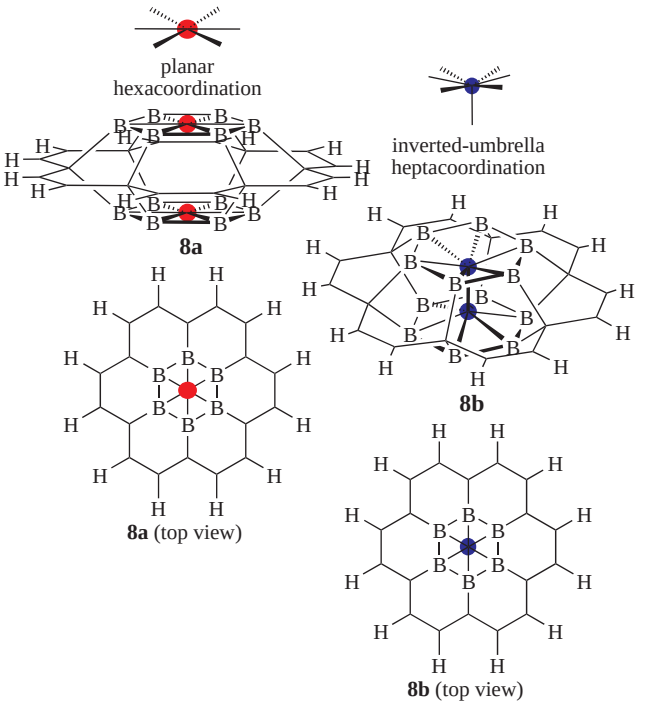


**Figure 1** Two non-classical states of the apical carbon atoms in system **8**: planar hexacoordination **8a** and inverted-umbrella heptacoordination **8b**. Red and blue circles represent planar hexacoordinated carbon and inverted-umbrella heptacoordinated carbon, respectively.

6-311+G(df,2p)[19] split-valence basis set using the Gaussian 16 program package.[20] Stationary points on potential energy surfaces (PESs) were located with full geometry optimization, identified by calculating the matrix of second derivatives (force constants) and checked for stability of the Hartree–Fock solution. The wave functions of all considered systems are stable. Natural bond orbital (NBO) analysis[21] was performed with the help of the NBO 6.0 program.[22] AIM (Atoms in Molecules) analysis[23] was carried out using the AIMAll Professional program.[24] The drawings were made using the ChemCraft program suite[25] with the calculated atomic coordinates as input parameters.

According to the calculations at both levels, system **8** can exist in two isomeric forms, **8a** and **8b**, which are characterized by $D_{6h}$ symmetry and correspond to energy minima ($\lambda$ = 0, hereinafter λ denotes the number of negative eigenvalues of the matrix of second derivatives) on the PES. The ground state of both isomers of system **8** is a closed-shell singlet. The triplet state is destabilized with respect to the singlet state by 33 (B3LYP) or 54 kcal mol$^{-1}$ (wb97XD) in the case of isomer **8a** and by 19 (B3LYP) or 30 kcal mol$^{-1}$ (wb97XD) in the case of isomer **8b**. Structural parameters of isomers **8a** and **8b** are shown in Figure 2, and their energy parameters are collected in Table S1 (see Online Supplementary Materials).

Isomers **8a** and **8b** differ in the degree of near nesting of $CB_6$ rings and in the configuration of carbon atom bonds. Form **8a** is characterized by markedly separated $CB_6$ fragments with a distance between the central carbon atoms of 2.484 (B3LYP) or 2.494 Å (wb97XD), while in form **8b** the $CB_6$ fragments are substantially drawn together, and the distances between carbon atoms are diminished to 1.387 (B3LYP) or 1.384 Å (wb97XD). Form **8b** is slightly more stable than form **8a**: the energy difference is 1.26 (B3LYP) or 3.04 kcal mol$^{-1}$ (wb97XD). Both isomers are characterized by high values of the first harmonic vibrational frequencies (from ~170 to 180 cm$^{-1}$), which indicates[26] their significant kinetic stability.

The central carbon atoms of the $CB_6$ units in form **8a** have almost planar bond configuration: pyramidalization is within ~5°, and the calculated CB bond lengths are 1.649 (B3LYP) or 1.648 Å (wb97XD). The CB bonds in isomer **8b** are noticeably longer than in isomer **8a** and are 1.746 (B3LYP) or 1.738 Å (wb97XD). The central carbon atoms in form **8b** are pyramidalized to a much greater extent than in form **8a**: according to both methods, the pyramidalization angle is ~29°.

Thus, form **8a** includes two quasi-planar hexacoordinated carbon atoms, while the carbon atoms in form **8b** are heptacoordinated and have an inverted-umbrella bond configuration. In addition to six bonds with surrounding boron atoms, carbon atoms in isomer **8b** form a central CC bond, the length of which is 1.387 (B3LYP) or 1.384 Å (wb97XD). The length of this bond is greatly reduced compared to the single carbon–carbon bond (1.54 Å)[27] and is close to the length of the double bond (1.34 Å).[27] The calculated Laplacian bond order (LBO)[28] for the central CC bond is 1.4 (B3LYP) or 1.5 (wb97XD), which also indicates a significant contribution of double bonding. For comparison, peripheral –CH=CH– bridges have similar parameters: their length is 1.360 (B3LYP) or 1.353 Å (wb97XD), and LBO is 1.7 (B3LYP) or 1.8 (wb97XD).

According to the AIM analysis (see molecular graphs in Figure 2), each carbon atom in system **8a** is linked by six bond paths to the boron environment, which indicates its hexacoordination. In system **8b**, carbon atoms form an additional, seventh, bond path corresponding to CC bonding, and thus are heptacoordinated. Each of the bond paths connecting carbon atoms with the boron environment in system **8** corresponds to the interaction of the carbon center with the BB bond, and not directly with single boron atoms.

Table S2 lists the calculated AIM parameters for the bond critical point (BCP) corresponding to CB interactions in system **8**. As can be seen from the table, the BCPs are characterized by negative values of the electronic Laplacian $\nabla^2\rho(r)$ attributed to covalent-type interactions. Additionally, the values of the charge density $\rho(r)$ at the BCP are large enough (0.15) and close to those for covalent single bonds (from ~0.25 to 0.30). At the same time, the negative sign of the total energy density $H(r)$ indicates the covalent nature of these interactions. When passing from form **8a** to form **8b**, the values of the charge density at the critical points of the CB bonds slightly decrease. This trend correlates with the lengthening of the CB bonds in form **8b** and indicates a weakening of the interaction. Another criterion to assess the

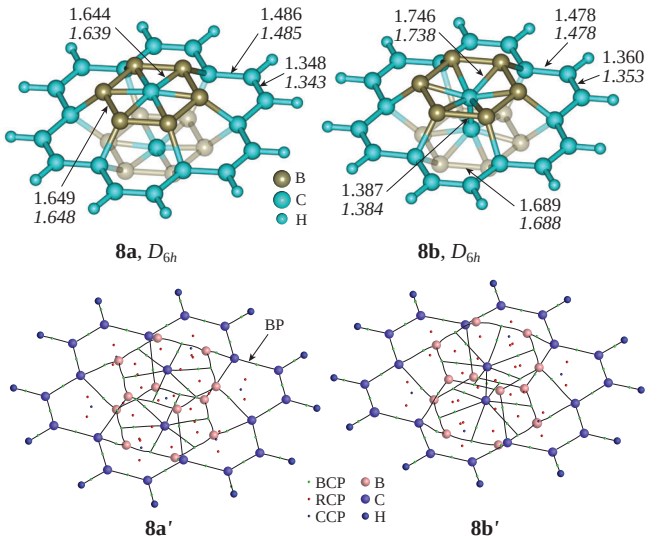


**Figure 2** Geometric characteristics (bond lengths, Å) of systems **8a** and **8b** calculated using the B3LYP and wb97XD (italicized values) methods with the 6-311+G(df,2p) basis set. The Bader molecular graphs **8a′** and **8b′** of structures **8a** and **8b**, respectively, are given at the bottom, BP designates the Bader bond path, CP – the bond path critical point, RCP – the ring critical point and CCP – the cage critical point.

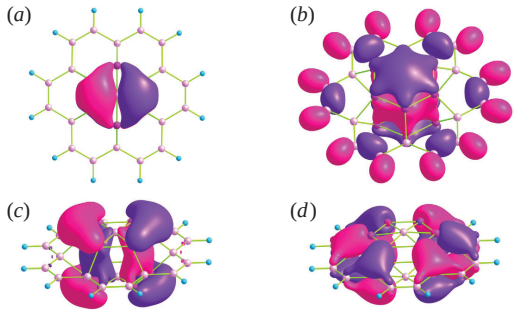


**Figure 3** Shapes of multicenter bonding molecular orbitals providing the formation of (*a*),(*b*) hypercoordinated nodes, (*c*) central CC double bond and (*d*) peripheral three-dimensional aromaticity in systems **8**.

nature of bonding is the ratio between the kinetic and potential energy densities $-G(r)/V(r)$.[29,30] For forms **8a** and **8b**, this value is less than 0.5, which points to a predominantly covalent interaction.

According to the results of molecular orbital and NBO analyzes, the formation of hypercoordinated carbon centers in systems **8a** and **8b** is provided by donating electron density from the bonding orbitals of BB bonds formed by the interaction of $sp^2$-hybridized boron orbitals (with a high contribution of the s-component) to the antibonding combination of *p* orbitals of two carbon atoms [Figure 3(*a*)]. In addition, back-donation occurs from unhybridized filled $p_z$ orbitals of carbon atoms to vacant $p_z$ orbitals of the boron environment [Figure 3(*b*)]. In system **8b**, the $p_z$ orbitals of carbon atoms are involved in the formation of the central CC bond, which leads to a decrease in the electron density donation from carbon atoms to the boron environment, weakening of the CB interaction and elongation of the corresponding bonds. The central π-bonding in system **8b** is provided by carbon *p* orbitals located in the basal planes, which simultaneously participate in the interaction with boron atoms [Figure 3(*c*)].

For the central CC bond in isomer **8b**, the calculated AIM parameters (negative electron density Laplacian and significant charge density at the critical point) also indicate the covalent nature of the bond. In this case, the value of the electron density at the BCP is 0.336, which exceeds the values typical of covalent single bonds. The $-G(r)/V(r)$ ratio for the BCP corresponding to the CC bond is 0.227, which points to an increase in the covalent component compared to the CB bonds.

The calculated BB distances along the perimeter of the $CB_6$ fragments are 1.644 (B3LYP) or 1.639 Å (wb97XD) for structure **8a** and 1.689 (B3LYP) or 1.688 Å (wb97XD) for structure **8b** and are significantly shortened compared to those for single covalent BB bonds (1.75 Å).[27] The strong BB bonding along the perimeter of the $CB_6$ fragments, as well as the rigidity of the framework, are additional factors for the stabilization of non-classical carbon centers.

As can be seen from Figure 2, the molecular graphs of isomers **8a** and **8b** are characterized by ring critical points (RCPs) and cage critical points (CCPs) indicating the aromaticity of these systems. The calculated NICS indices[31] corresponding to the CCPs ($NICS_{CCP}$) located in the center of the molecules have high negative values [–58.9 (B3LYP) or –60.0 ppm (wb97XD) for isomer **8a** and –39.1 (B3LYP) or –41.0 ppm (wb97XD) for isomer **8b**], which are characteristic of diatropic ring currents in these regions and the three-dimensional aromaticity of system **8**. In the peripheral sectors of the hydrocarbon linker, the calculated values of the $NICS_{CCP}$ indices corresponding to the CCPs and located at the central points of the C···C axes are also negative [–7.6 (B3LYP) or –7.2 ppm (wb97XD) for isomer **8a** and –5.7 (B3LYP) or –5.8 ppm (wb97XD) for isomer **8b**], which points to the local 3D aromaticity of the peripheral environment. According to molecular orbital analysis, the 3D aromaticity of systems **8** is provided by spatial overlapping of the upper and lower π-systems of the $CB_6$ units [Figure 3(*b*),(*c*)], as well as π-systems of hydrocarbon linker fragments [Figure 3(*d*)]. The stacking interaction between the basal π-systems in isomer **8b** is accompanied by the formation of a covalent bond, similarly to how it occurs in systems with pancake bonding.[32] However, in contrast to pancake-bonded systems, the covalent bond in isomer **8b** has a high degree of double bond character.

Isomers **8a** and **8b** are separated by an energy barrier high enough to isolate individual non-classical forms. According to calculations, the barrier for the isomerization of form **8a** to form **8b** is 29.4 (B3LYP) or 25.3 kcal $mol^{-1}$ (wb97XD). The structure of transition state **9** is characterized by $C_{6v}$ symmetry and includes two non-classical hexacoordinated carbon centers, one of which is planar (as in isomer **8a**) and the other is pyramidal. The distance between the two centers is 1.869 (B3LYP) or 1.948 Å (wb97XD). In the transition state, three-dimensional aromaticity is lost due to symmetry breaking about the plane perpendicular to the main axis, which leads to an increase in the isomerization barrier.

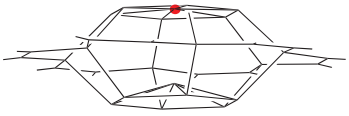

**9**

An important feature of systems **8** is the possibility of forming on their basis complex condensed derivatives with a regular structure **10** as surfaces, extended ribbons or hole-type systems, including many non-classical hypercoordinated carbon atoms in various forms. Similarly composed three-layer structures contain non-classical units in the basal layers with a hydrocarbon interlayer between them. Calculations carried out for the simplest trimeric derivatives **11** showed that these condensed systems correspond to energy minima ($\lambda = 0$) on the PES. Like the initial monomers **8**, system **11** has isomeric forms with planar hexacoordinated and inverted-umbrella heptacoordinated carbon atoms (Figure 4).

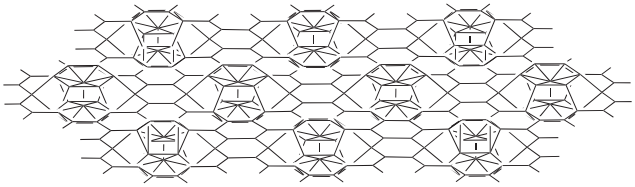

**10**

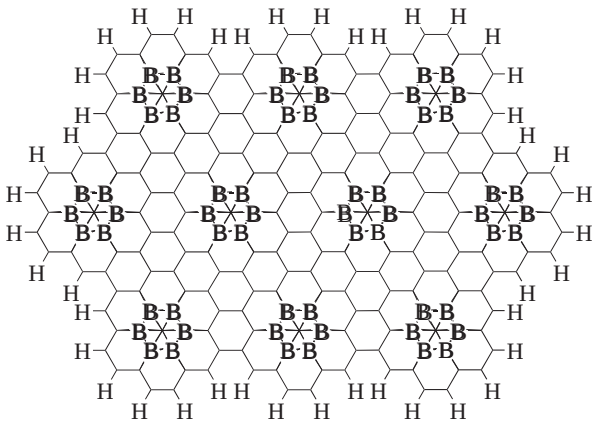

**10** (top view)

Isomers **11a** and **11b** are constructed from three blocks **8a** and **8b**, respectively, and thus contain six planar hexacoordinated (isomer **11a**) and six inverted-umbrella heptacoordinated (isomer **11b**) carbon centers. Forms **11c** and **11d** are built from two types of structural blocks and simultaneously include non-

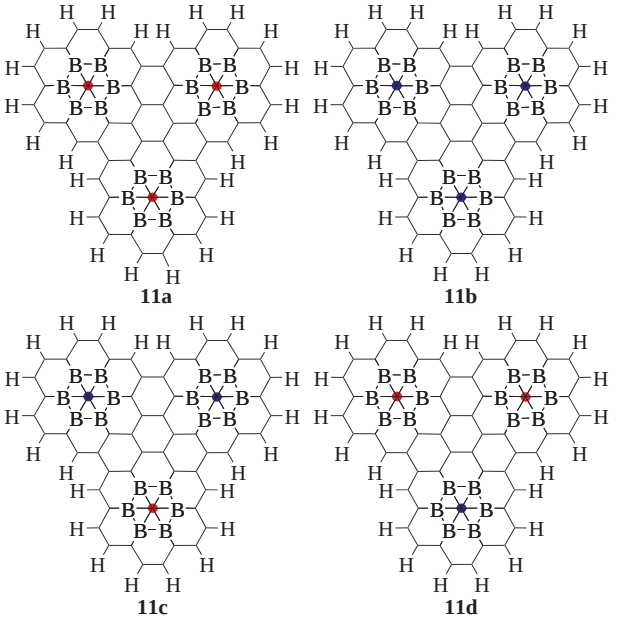


**Figure 4** Isomeric forms of system **11** containing planar hexacoordinated (red circles) and inverted-umbrella heptacoordinated (blue circles) carbon atoms.

classical carbon centers in two hypercoordination states. Isomer **11c** includes two blocks **8a** and one block **8b** and contains four planar hexacoordinated and two inverted-umbrella heptacoordinated carbon centers. Isomer **11d**, constructed from one block **8a** and two blocks **8b**, contains two planar hexacoordinated and four inverted-umbrella heptacoordinated carbon centers.

As in the case of the simplest derivatives **8**, isomer **11b**, containing only inverted-umbrella heptacoordinated centers, is the most energetically preferable. The thermodynamic stability of the isomeric forms decreases in the series **11b** > **11c** > **11d** >**11a** with an increase in the number of the planar hexacoordinated carbon centers. Isomer **11a**, which includes only planar hexacoordinated carbon centers, is the least energetically favorable. The energy preference of form **11b** with only heptacoordinated carbon relative to form **11a** with only hexacoordinated carbon increases compared to derivatives **8** and is 15.50 (B3LYP) or 13.23 kcal mol$^{-1}$ (wb97XD). The formation of complicated systems has practically no effect on the geometric characteristics of the structural blocks in the monomeric unit. The structural and energy parameters of isomers **11a** and **11b** are presented in Figure S5 and Table S1.

In summary, the performed calculations predict the stability of organoboron species **8**, which are a new type of non-classical structures with carbon atoms in two states of hypercoordination: planar hexacoordination and inverted-umbrella heptacoordination. Systems **8** are stabilized by both steric and electronic effects (rigid framework, boron substituents effect and 3D aromaticity) and can serve as structural blocks for the formation of stable condensed associates containing a sequence of many non-classical carbon centers of different types.

This work was supported by the Ministry of Science and Higher Education of the Russian Federation within the framework of the State Assignment in the field of scientific activity to the Southern Federal University (project no. 0852-2020-0019).

*Online Supplementary Materials*

Supplementary data associated with this article can be found in the online version at doi: 10.1016/j.mencom.2022.05.002.

## References

1 V. I. Minkin, R. M. Minyaev and R. Hoffmann, *Russ. Chem. Rev.*, 2002, **71**, 869.
2 Y. Wang, Y. Li and Z. Chen, *Acc. Chem. Res.*, 2020, **53**, 887.
3 R. Keese, *Chem. Rev.*, 2006, **106**, 4787.
4 L.-M. Yang, E. Ganz, Z. Chen, Z.-X. Wang and P. von Ragué Schleyer, *Angew. Chem., Int. Ed.*, 2015, **54**, 9468.
5 V. Vassilev-Galindo, S. Pan, K. J. Donald and G. Merino, *Nat. Rev. Chem.*, 2018, **2**, 0114.
6 P. von Ragué Schleyer and A. I. Boldyrev, *J. Chem. Soc., Chem. Commun.*, 1991, 1536.
7 R. M. Minyaev, T. N. Gribanova and V. I. Minkin, in *Comprehensive Inorganic Chemistry II: From Elements to Applications*, eds. J. Reedijk and K. Poeppelmeier, Elsevier, Amsterdam, 2013, vol. 9, pp. 109–132.
8 T. N. Gribanova, R. M. Minyaev and V. I. Minkin, *Russ. J. Gen. Chem.*, 2008, **78**, 750 (*Ross. Khim. Zh.*, 2007, **51**, 71).
9 Z.-X. Wang and P. von Ragué Schleyer, *Science*, 2001, **292**, 2465.
10 K. Exner and P. von Ragué Schleyer, *Science*, 2000, **290**, 1937.
11 R. M. Minyaev, T. N. Gribanova, A. G. Starikov and V. I. Minkin, *Dokl. Chem.*, 2002, **382**, 41 (*Dokl. Akad. Nauk*, 2002, **382**, 785).
12 R. M. Minyaev, T. N. Gribanova, A. G. Starikov and V. I. Minkin, *Mendeleev Commun.*, 2001, **11**, 213.
13 S.-D. Li, J.-C. Guo, C.-Q. Miao and G.-M. Ren, *Angew. Chem., Int. Ed.*, 2005, **44**, 2158.
14 Q. Luo, X. H. Zhang, K. L. Huang, S. Q. Liu, Z. H. Yu and Q. S. Li, *J. Phys. Chem. A*, 2007, **111**, 2930.
15 Y. Wang, F. Li, Y. Li and Z. Chen, *Nat. Commun.*, 2016, **7**, 11488.
16 K. H. Yeoh, K.-H. Chew, Y. Z. Chu, T. L Yoon, Rusi and D. S. Ong, *J. Appl. Phys.*, 2019, **126**, 125302.
17 A. D. Becke, *J. Chem. Phys.*, 1993, **98**, 5648.
18 J.-D. Chai and M. Head-Gordon, *Phys. Chem. Chem. Phys.*, 2008, **10**, 6615.
19 J. B. Foresman and Æ. Frisch, *Exploring Chemistry with Electronic Structure Methods*, 2nd edn., Gaussian, Inc., Pittsburgh, 1996.
20 M. J. Frisch, G. W. Trucks, H. B. Schlegel, G. E. Scuseria, M. A. Robb, J. R. Cheeseman, G. Scalmani, V. Barone, G. A. Petersson, H. Nakatsuji, X. Li, M. Caricato, A. V. Marenich, J. Bloino, B. G. Janesko, R. Gomperts, B. Mennucci, H. P. Hratchian, J. V. Ortiz, A. F. Izmaylov, J. L. Sonnenberg, D. Williams-Young, F. Ding, F. Lipparini, F. Egidi, J. Goings, B. Peng, A. Petrone, T. Henderson, D. Ranasinghe, V. G. Zakrzewski, J. Gao, N. Rega, G. Zheng, W. Liang, M. Hada, M. Ehara, K. Toyota, R. Fukuda, J. Hasegawa, M. Ishida, T. Nakajima, Y. Honda, O. Kitao, H. Nakai, T. Vreven, K. Throssell, J. A. Montgomery, Jr., J. E. Peralta, F. Ogliaro, M. J. Bearpark, J. J. Heyd, E. N. Brothers, K. N. Kudin, V. N. Staroverov, T. A. Keith, R. Kobayashi, J. Normand, K. Raghavachari, A. P. Rendell, J. C. Burant, S. S. Iyengar, J. Tomasi, M. Cossi, J. M. Millam, M. Klene, C. Adamo, R. Cammi, J. W. Ochterski, R. L. Martin, K. Morokuma, O. Farkas, J. B. Foresman and D. J. Fox, *Gaussian 16, Revision C.01*, Gaussian, Inc., Wallingford, CT, 2016.
21 A. E. Reed, L. A. Curtiss and F. Weinhold, *Chem. Rev.*, 1988, **88**, 899.
22 E. D. Glendening, J. K. Badenhoop, A. E. Reed, J. E. Carpenter, J. A. Bohmann, C. M. Morales, C. R. Landis and F. Weinhold, *NBO 6.0*, University of Wisconsin, Madison, 2013.
23 R. F. W. Bader, *Atoms in Molecules: A Quantum Theory*, Clarendon Press, Oxford, 1990.
24 T. A. Keith, *AIMAll, version 11.06.19*, TK Gristmill Software, Overland Park, USA, 2011.
25 G. A. Zhurko, *ChemCraft software, version 1.8*, http://www.chemcraftprog.com.
26 R. Hoffmann, P. von Ragué Schleyer and H. F. Schaefer, III, *Angew. Chem., Int. Ed.*, 2008, **47**, 7164.
27 J. Emsley, *The Elements*, Clarendon Press, Oxford, 1991.
28 T. Lu and F. Chen, *J. Phys. Chem. A*, 2013, **117**, 3100.
29 S. Shaik, D. Danovich, B. Silvi, D. L. Lauvergnat and P. C. Hiberty, *Chem. – Eur. J.*, 2005, **11**, 6358.
30 S. Shaik, D. Danovich, W. Wu and P. C. Hiberty, *Nat. Chem.*, 2009, **1**, 443.
31 P. von Ragué Schleyer, C. Maerker, A. Dransfeld, H. Jiao and N. J. R. van Eikema Hommes, *J. Am. Chem. Soc.*, 1996, **118**, 6317.
32 M. Kertesz, *Chem. – Eur. J.*, 2019, **25**, 400.

*Received: 14th October 2021; Com. 21/6724*